

Technical Article

Microstructural Investigations and Fracture Analysis of a Multi-Layer Al Panel of a Crashed Aircraft

H.R. Faridi¹, A. Momeni^{1,*}, M. Mohammadpour¹, V.Sarfarazi²

¹Department of Materials Science and Engineering, Hamedan University of Technology, Hamedan, Iran

²Department of Mining Engineering, Hamedan University of Technology, Hamedan, Iran

Received: 26 September 2017 - Accepted: 10 January 2018

Abstract

In this paper, the failure analysis was performed on a crashed airplane trunk sample. Received sample was composed of five different layers; Al 2024 as outer layer, a nearly pure Al clad, an anodized layer, an isolating material and the alloy 413 as interior layer. Macro and micro-cracks in the sample were mostly initiated from the areas close to or around the rivets. These cracks initiated in anodized layer, got through the cladding and entered into the outer Al 2024. Few corrosion sites similar to crevice were also observed behind the rivets and between isolating and cladding layers. It was found that the crevice corrosion and fatigue were responsible to form micro-cracks at these sites. Microstructural observations of Al 2024 layer showed that the micro-cracks were mostly initiated from inside out then they progressed through the interfaces of second phase particles and the matrix. It was found that larger particles were in favor of crack propagation along their interfaces. Second phase large particles are attributed to over-aging of trunk sample which was subjected to excessive heat from the engines.

Keywords: Aluminum 2024, Aging; Fractography, Crevice Corrosion, Fatigue, Crack Propagation

1. Introduction

Failure analysis and the preventions are important for all of the engineering disciplines. Material engineers often play a lead role in analyzing the failures, whether a component or an instrument fails in service or if it occurs in a manufacturing process. One of the most important applications for failure analysis involves the aerospace industry. Aluminum alloys are the best selection amongst metallic materials for the construction of airplanes due to their unique properties [1-4]. Although resistance to corrosion is an outstanding property of Al alloys, but low specific strength for some could be a major drawback for them. For this reason, other alloying elements such as Cu and Mg are added to increase Al strength through solid solution or precipitation mechanisms. Series 2xxx and 7xxx are groups of Al alloys that widely used to manufacture airplane trunks and parts due to their good combination of strength, corrosion resistance and low weight. Assessments on these alloys life times by considering different sources of failures such as corrosion, fatigue, and fracture have been the topics of many works [5-8]. To improve strength and therefore fatigue and fracture resistance in these alloys, different aging treatments have been advised [9, 10]. Despite positive influences of second-phase particles on the strength attributed to Al alloys, they increase the risk of failure by introducing more

potential sites for crack formation.

Given the general perception about the natural Resistance of Al alloys against corrosion, it has been proved that corrosion is a detrimental player for the airplanes structure due to their harsh working environment [11,12]. For this reason, different protecting prescriptions such as the cladding of constructional materials with more resisting ones, anodizing and so on have been proposed [13,14]. However, there are still controversies over the usefulness of these remedies for harsh conditions of flights where corrosion, fatigue and even creep may play roles simultaneously [15]. It is therefore clearly elicited that given fundamental investigations hitherto conducted in the corrosion, fatigue and fracture of airplane structural materials, more case studied would be helpful.

Present investigation carried out on real crashed airplane sample comprised of five layers. Failure analysis of sample by taking into account the synergistic effects of different corrosion mechanisms, fatigue, microstructural evolutions and some design perceptions such as; materials selection, surface protecting mechanism, riveting and other potential risks.

2. Materials and Methods

Some pieces of an airplane body were collected at the site of the crash. The samples were chosen from the pieces, near the area close to the engine. Selected sample was carried to the laboratory and used for further evaluations. After visual inspections, to determine the elemental compositions of sample, it

*Corresponding author

Email address: momeni@hut.ac.ir

was tested using an X-ray analyzer was conducted using by GNR Diffractometer (APD 2000) with Cu K radiation with 40 kV operating voltage, 30 mA current and 0.05 2 θ s⁻¹ scan rate. Before performing any destructive investigations, the fractured surfaces were also examined using JEOL JSM 5800 scanning electron microscope (SEM). To characterize microstructural features, sample was prepared by standard metallographic technique. After revealing the microstructure by the Keller's reagent, optical and scanning electron microscopy besides energy dispersive spectroscopy (EDS) were employed to characterize the observed microstructures.

3. Results and Discussion

3.1. Materials Characterization

Fig. 1. shows visual inspection of received sample. Pictures depict that the part was completely deformed due to the crashing and excessive heat induced from the crash site or even during the service. It may have assisted cracking associated with rivets, (Figs. 1(b) and (c)).

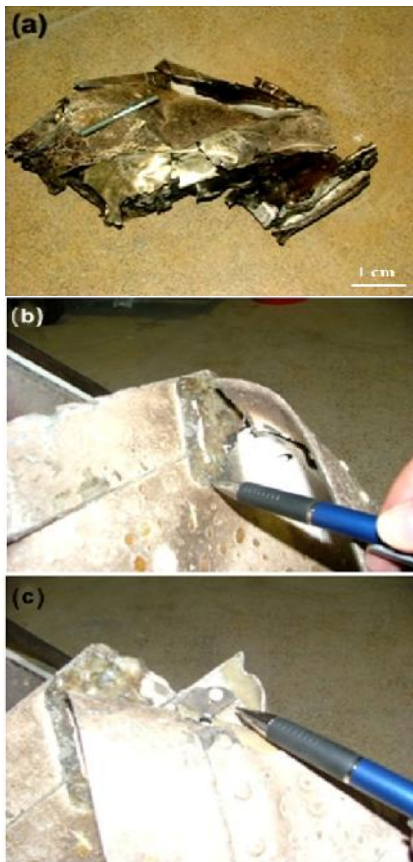


Fig. 1. Visual inspection of (a) received sample, (b) and (c) magnified views of (a).

Fig. 2. shows a mounted sample, prepared by metallographic techniques.

Riveting on received sample was selected for further microstructural investigations because visual inspections, as in Fig. 1(c), showed that they might have been responsible for cracking.

Fig. 3. presents optical microscopy of prepared sample, revealing an insulating polymeric layer, visible as a dark layer, separates the outer section of trunk, denoted as part 1, from the interior, denoted as part 2. It is clear that each part is characterized by different microstructural features which should be separately analyzed.

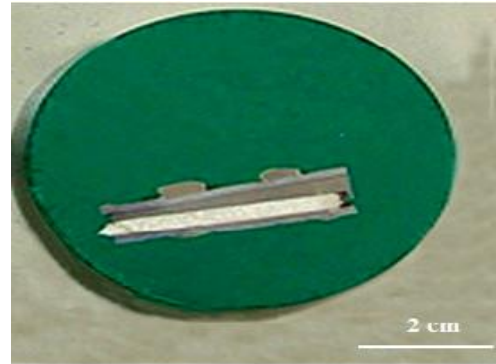


Fig. 2. Selected section of received sample mounted for metallographic preparation.

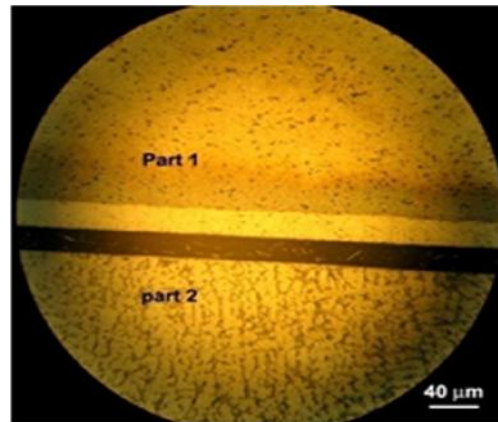


Fig. 3. Image of the sample showed in, Figure 2, optical microscopy of different layers.

Fig. 4. shows the SEM micrograph of part 1, seen on Fig. 3. Micrograph depicts that the sample seems to be composed only in 4 layers, denoted as L1 to L4, from outer surface of the airplane trunk inward. Layer indicated by L4 is the polymeric insulating layer between outer (part 1) and inner (part 2) of the airplane trunk. This layer is crucial to avoid sound and heat get in or out of the airplane cabin. In order to characterize the underneath layers (L1, L2 and L3), individual EDS analyses were carried out.

Fig. 5. shows the EDS analysis of layer L1, seen on Fig. 4.

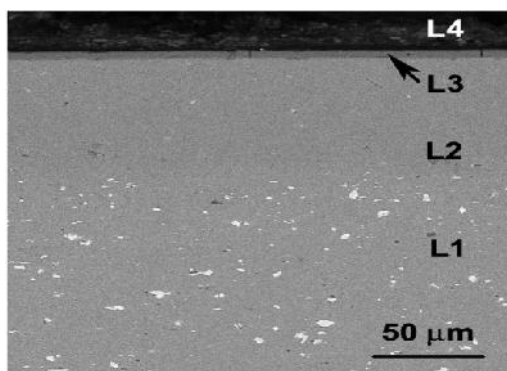


Fig. 4. SEM micrograph of part1, representing four different layers.

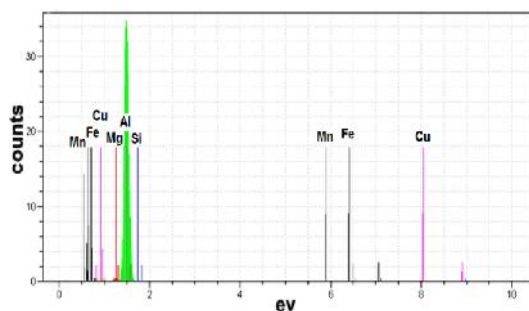


Fig. 5. EDS results of layer L1, seen on Fig. 4.

Table 1 given the summarizes quantitative analysis of L1 in comparison with the standard composition of Al 2024 alloy, which is a very common alloy for an aircraft trunk construction.

Fig. 6. shows a magnified SEM micrograph of layer L1 and EDS analysis of second phase particles. According to the results, the precipitated phase is composed of about 55.8 wt. % Cu, 33.6 wt. % Al and 10.5 wt. % Mg complying with a non-stoichiometric compound, the CuMgAl_2 . These precipitates are usually formed in Al 2024 aging heat treatment process as a major source of alloy strengthening [16, 17].

Table. 1. Quantitative elemental analysis from the sample in comparison with standard Al 2024 alloy (wt. %).

Sample	Layer L1	Al 2024
Al	Base	Base
Ti	0.050	0.150
Zn	0.030	0.250
Cr	0.007	0.100
Mg	1.290	1.200– 1.800
Mn	0.410	0.300 – 0.900
Cu	4.390	3.800- 4.900
Fe	0.190	0.500
Si	0.190	0.500

Through the aging process of Al 2024, a big portion of hardening (actually about 70%) is achieved when the solute atoms of Cu and Mg co-cluster [18].

Further aging gives rise to gradual formation of S phase with the formula CuMgAl_2 , imparting more strength to the alloy. As the size of S particles increases by over-aging, the rate of hardening decreases and the alloy eventually weakens.

Over-aging occurs not only in a prolonged aging treatment, but it also can develop during service at high temperatures. This phenomenon is undesirable and the weakened alloy should be rejuvenated by a new cycle of solution treatment and aging. Furthermore, due to the presence of Si, Fe, and Mn in Al 2024, formation of other detrimental phases such as Mg_2Si , $\text{Cu}_2\text{Mg}_8\text{Si}_5\text{Al}_4$, and $(\text{Cu, Fe, Mn})\text{Al}_6$ would also be expected during prolonged aging or exposure to high temperatures at service.

In the SEM micrographs of Figs. 4. and Fig. 6., a distribution of second phase particles within the size range of 1 to 8 micron can be observed in L1.

It seems that some particles have grown in service, presumably due to exposing to high temperatures of the engines. As mentioned before, coarsening of second phase particles will decrease the strength as well as fracture toughness of the alloy.

The coarsen particles particularly increase the stress concentration factors and might lead to a premature cracking.

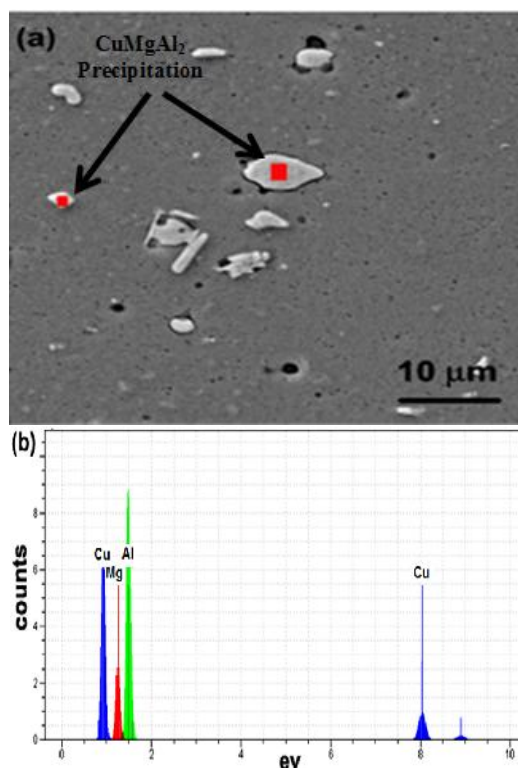


Fig. 6. (a) Magnified SEM micrograph of layer L1 seen on Fig. 3., (b) EDS analysis of selected particles in (a).

EDS analysis of the second layer (L2), shown in Fig. 7., indicates that this layer is mostly composed of Al (99.6 wt. %) with about 0.4 wt. % of Si. Therefore, this inferred that L2 is a clad layer of nearly pure Al on L1.

The clad surface is resistant to corrosive attack and also provides additional cathodic protection to Al 2024 layer [19]. As observed in Fig. 3., a part of layer L1, adjacent to L2, has been heat-colored due to cladding process. Although, the clad layer increases corrosion resistance of Al 2024 but different thermal and mechanical properties for L1 and L2 potentially increases the risk of premature fracture due to thermo-mechanical fatigue. This should be taken more seriously into consideration for areas near the engines, where excessive heating and cooling cycles are engaged.

EDS analysis of L3 in Fig. 8. indicates that, this is an anodized layer performing as top metallic layer (below the insulation) to protect underneath layers from possible corrosive environments from inside. Analysis result depicted that anodize layer is mainly consisted of 67.7 wt. % Al, 25.5 wt. % O₂ and about 7 wt. % of S.

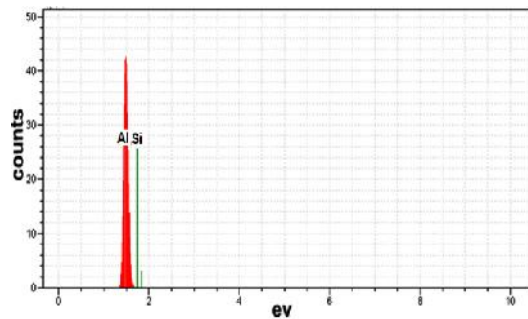


Fig. 7. EDS analysis of layer L2, seen on Fig. 4.

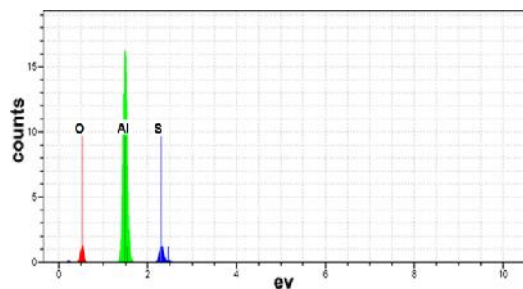


Fig. 8. EDS analysis of the layer L3 seen on Fig. 4.

Microstructural image and the EDS analysis of part 2, seen on Fig. 3., are shown in Fig. 9. EDS analysis showed that this layer is mostly composed of about 86.5 wt. % of Al, 13 wt. % of Si, Fe and Mg as the remainder. The analysis actually complies with Al-Si casting alloys (especially alloy 413) consisted of a matrix rich in Al and shapeless Si islands [20]. It is known well that the silicon particles in such alloys tend to form globular when aged or subjected to heat

in service. This would be other symptom for sections of trunk near the airplane engines. It is also worthy to mention that some micro-cracks are visible within Si particles. Pointed particles on Fig. 9. (a) show that, cleavage micro-cracks may have formed before or even during the crash. It is clear that if the material was subjected to high temperatures for long time, silicon particles tended to agglomerate and form larger spherical ones. This in turn increases the tendency for cleavage cracking which may have propagated through particles..

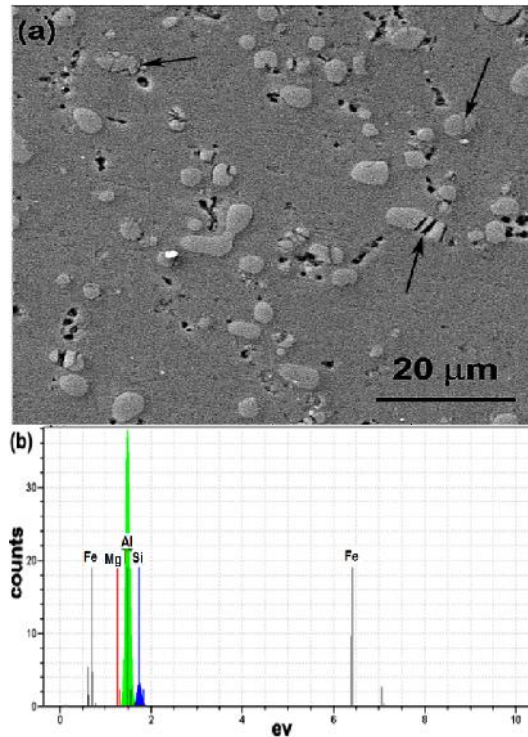


Fig. 9. (a) Magnified SEM image, and (b) EDS analysis of Part2, seen on Fig. 3.

3.2. Failure Behavior and Fractography

Failure analysis on the airplane body part was focused on the fracturing because of possible corrosion and the fatigue because of working conditions. Part actually was subjected to overheating which may have caused coarsening in Cu-Mg particles in Al 2024 alloy (layer L1) and the Si particles in alloy 413 (layer L5). In addition, cyclic heating and cooling of part increased risk of thermo-mechanical fatigue. It is worthy to mention that corrosion played detrimental roles, particularly when stresses are intensified in areas adjacent to rivets [8]. Fig. 10. shows cracking emerged in layers L2 and L3 close to a rivet.

Fig. 10 (a). shows that a crack has initiated from a crevice corrosion position under a rivet and the stress concentration field around it caused its propagation into layer L2. In Fig. 10 (b)., crevice corrosion is

observed in interlayer region between L2 and L4. Corrosion is ruining the protective anodize layer (L3) and advancing into layer L2. This is potentially a weak position for cracking as shown in Fig. 10 (a). Existing stress concentration fields around the rivets making the condition more severe in regards with crack initiation and propagation, as in Fig. 10 (a).

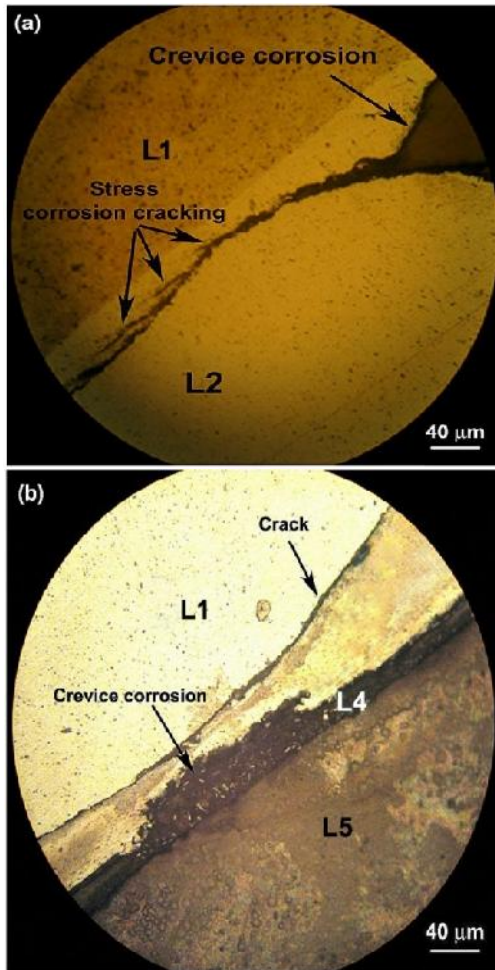


Fig. 10. (a,b) Optical microscopic imaging of cracks and crevice corrosion at two positions behind a rivet.

Fig. 10 (b). shows that at some positions cracks may adopt a way into layer L1 instead. These positions are where the material is subjected to engines heating and the precipitates in layer L1 tended to become coarser [21]. Coarsening is usually accompanied by changing interface with matrix into incoherent state making the material locally susceptible to cracking. At such condition, not only the strength decreases, but the fracture toughness degrades as well. In a material with coarsened particles, the interphase interfaces will be prone to incoherency and cracking. This is demonstrated clearly in Fig. 11.

Showing a magnified SEM image of a crack propagated in layer L1.

Based on microstructural investigations, it would be fair to say that any sections of the trunk which was not subjected to over-heating by the engines has maintained its integrity with no crack propagation in Al 2024 layer even around the rivets. In such locations, major reason for cracking would be the synergistic effects of crevice corrosion and stress concentration fields around the rivets. In a way, fine dispersion of any second phase particles could effectively prohibit cracking in either external or internal layers. But, coarsened particles in both alloys could be harmful to the fracture toughness of trunk. Seemingly, larger the particle has less adhesion to matrix in both layers, by enforcing even more susceptibility to cleavage in alloy 413 along its border line and the matrix.

Fig. 12. shows two SEM micrographs of fracture surface between layers L2 and L3 in different magnifications. Faceted fracture surface within L3 is a sign of its brittleness, unlike the L2 which can be characterized by a fibrous ductile fracture appearance.

Different fracture features for these layers could have been related directly to their chemical compositions and microstructures. Micro-cracks appeared in L3 adjacent to the interfaces may be caused by thermo-mechanical fatigue due to different thermal properties of the layers. The fracture surface in layer L1 is represented in Fig. 13. Fibrous appearance of the failed surface with small dimples implies that the material has undergone plastic deformation before fracture.

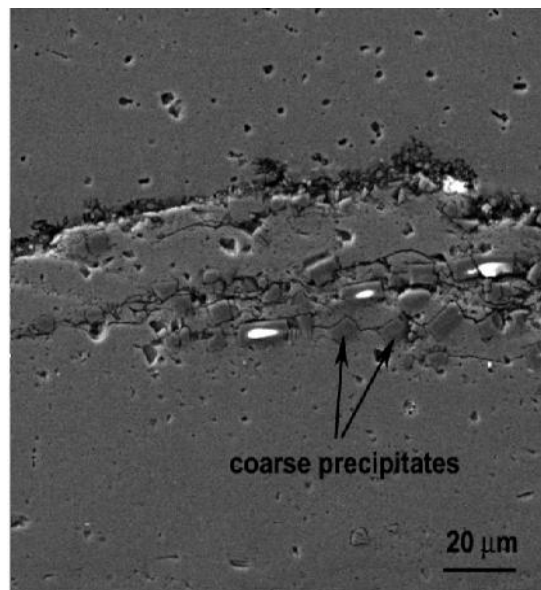


Fig. 11. SEM micrograph of crack propagation in layer L3 in favor of coarse precipitates formed during heating.

It is also worthy to mention that some of these dimples, most possibly those pointed by arrows contains large second-phase particles.

This fortifies the previous observations, as in Fig. 13.,

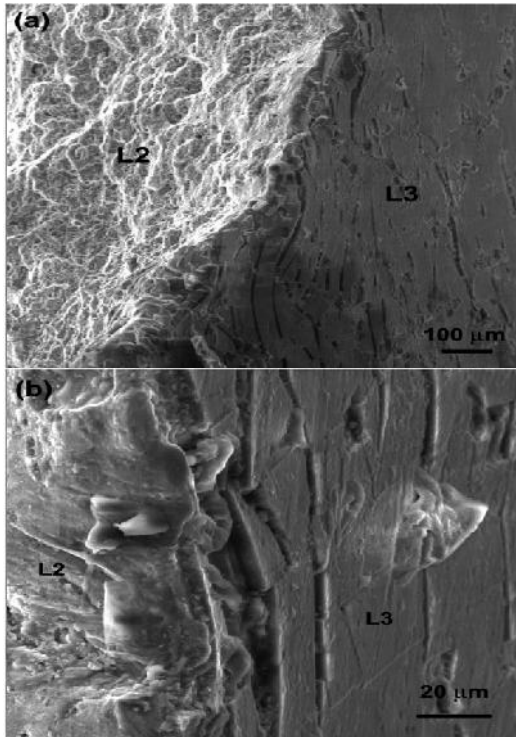


Fig. 12. (a,b) SEM micrograph of a failed cross section between layer L2 and L3.

and highlights the contributions of coarsened particles on the micro cracks initiations final fracturing.

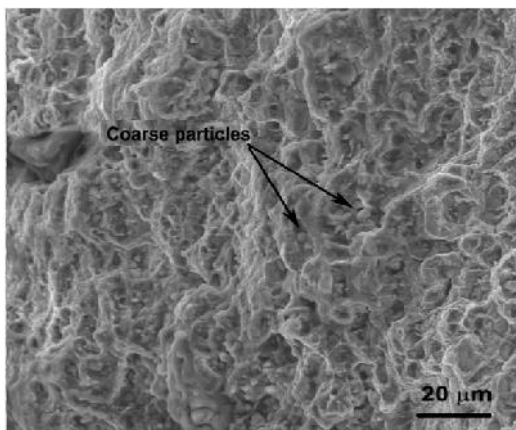


Fig. 13. SEM micrograph of a fracture surface within layer L1.

4. Conclusions

1. Sample was composed of five layers from the outside in; Al 2024, nearly pure Al clad, anodized layer, isolating material and alloy 413.
2. Cracks and micro-cracks found on sample were mostly initiated from inside and around the rivets, entering to outer layer by advancing through the anodized and cladding.
3. Few corrosion sites similar to crevice corrosion were observed behind the rivets and between the isolating and cladding layers. It would be fair to say that a combination of crevice corrosion and thermo-mechanical fatigue caused the cracking.
4. Microstructural observations of Al 2024 layer showed that micro-cracks were mostly initiated from inside and then progressed through the second phase interfaces with the matrix. It was found that larger particles could favor the crack propagation along their border line with the matrix. Having large particles was attributed to over-aging some section of trunk which was subjected to the engines heating.

References

- [1] C. Svoboda, *Sci. Aircr. Des.*, 2(1999), 231.
- [2] L.D. Hefti, *J. Mater. Eng. Perform.*, 16(2007), 136.
- [3] E.A. Starke Jr. J.T. Staley *Prog. Aerosp. Sci.* Elsevier, (2011), 747.
- [4] E.V. Abolikhina and A.G. Molyar, *Mater. Sci.*, 39(2003), 889.
- [5] P. Sivaraj, D. Kanagarajan and V. Balasubramanian, *Trans. Nonferrous Met. Soc. China*, 24(2014), 2459.
- [6] Al.Th. Kermandis, P.V. Petroyiannis and Sp.G. Pantelakis, *Theor. Appl. Fracture Mech.*, 43(2005), 82.
- [7] G.-Z. Quan, F.-B. Wang, Y.-Y. Liu, Y. Shi and J. Zhou, *Trans. Nonferrous Met. Soc. China*, 23(2013), 749.
- [8] B. Zhang, C. Tao and C. Liu, *Eng. Failure Analysis*, 35(2013), 82.
- [9] S. Liu, S. Li, S. Han, Y. Deng and X. Zhang, *J. alloys Comp.*, 625(2015), 34.
- [10] P.A. Rometsch, Y. Zhang and S. Knight, *Trans. Nonferrous Met. Soc. China*, 24(2014), 2003.
- [11] T. Mills, S. Prost-Domasky, K. Honeykott and C. Brooks, *Corrosion Control in the Aerospace Industry*, (2009), 35.
- [12] L. Molent L, *Eng. Fracture Mech.*, 137(2015), 12.
- [13] Sp.G. Pantelakis, A.N. Chamos and D. SEtsika, *Theor. App. Fracture Mech.*, 58(2012), 55.
- [14] B.N. Parker., *Int. J. Adhesion and Adhesives*, 1 (1980), 23.
- [15] Sp.G. Pantelakis, A.N. Chamos and Al.Th. Kermandis, *Theor. Appl. Fracture Mech.*, 57(2012), 36.
- [16] Y.C. Lin, Y.-C. Xia, Y.-Q. Jiang, H.-M. Zhou and L.-T. Li, *Mater. Sci. Eng.*, A565(2013), 420.

- [17] F.-S. Xu, J. Zhang, Y.-L. Deng and X.-M. Zhang , Trans. Nonferrous Met. Soc. China, 24(2014), 2067.
- [18] S.P. Ringer, T. Sahura and I.J. Polmear, Acta Mater., 45(1997), 3731.
- [19] D.T. Parker, Building Victory: Aircraft Manufacturing in the Los Angeles Area in World War II. Cypress, CA, (2013).
- [20] M. Warmuzek, Aluminum-silicon Casting Alloys: Atlas of Microfractographs. ASM International, 2004, 107.
- [21] Z. Feng, Y. Yang, B. Huang, M. Han, X. Luo and J. Ru , Mater. Sci. Eng., A528(2010), 706.

